Geometry and Energetics of CO Adsorption on Hydroxylated UiO-66

Journal:	*Physical Chemistry Chemical Physics*
Manuscript ID	CP-ART-12-2018-007778.R2
Article Type:	Paper
Date Submitted by the Author:	04-Feb-2019

Complete List of Authors:	Driscoll, Darren; Virginia Tech, Chemistry Troya, Diego; Virginia Tech, Chemistry Usov, Pavel; Virginia Tech, Chemistry Maynes, Andrew; Virginia Tech, Chemistry Morris, Amanda; Virginia Tech, Chemistry Morris, John; Virginia Tech, Department of Chemistry (MC 0212)

Geometry and Energetics of CO Adsorption on Hydroxylated UiO-66

Darren M. Driscoll, Diego Troya, Pavel M. Usov[1], Andrew J. Maynes, Amanda J. Morris, John R. Morris*

Department of Chemistry, Virginia Tech, Blacksburg, Virginia 24061, United States

*corresponding author email address: jrmorris@vt.edu

[1]Present address: Department of Chemistry, School of Science, Tokyo Institute of Technology, 2-12-1 Ookayama, Meguro-ku, Tokyo 152-8550, Japan

ORCID:
Darren M. Driscoll: 0000-0001-8859-8016
Diego Troya: 0000-0003-4971-4998
Andrew J. Maynes: 0000-0001-5084-4517
Amanda J. Morris: 0000-0002-3512-0366
John R. Morris: 0000-0001-9140-5211

Abstract

The metal-organic framework (MOF), UiO-66, contains Brønsted acidic and Lewis acidic sites that play an important role in sorption, separation, and potential catalytic processes involving small gaseous molecules. In particular, the sequestration and separation of CO within UiO-66 provides a fundamental understanding of small gas molecule adsorption within a highly porous, tunable and environmentally stable MOF. Infrared spectroscopic measurements, in combination with density functional theory, were employed to characterize the binding energetics between bridging hydroxyl groups at MOF nodes and the adsorbate, CO. Two unique binding configurations between CO and the μ_3-OH groups were identified based on differing stretching vibrations of $\nu(CO)_{ads}$ when interacting through the C- and O- atom of the molecule. Variable temperature infrared spectroscopy (VTIR) was employed to attain energetics of CO adsorption (-17 kJ/mol) and isomerization from the carbonyl to the isocarbonyl configuration (4 kJ/mol). Results suggest that CO-hydroxyl interactions, while weak in nature, are required for CO adsorption within the confined pore environment of UiO-66.

Introduction

Zirconium-based metal-organic frameworks (MOFs) are a promising class of materials that exhibit a unique blend of structural stability and tunability useful for gas adsorption, separation, and catalysis.[1,2] The Zr-MOFs are well known to retain their porous structure upon the introduction of significant defects, including both missing linker and missing node defects, and ligand modification.[3-5] In addition, the Zr-MOFs chemical heterogeneity generates an abundance of Lewis acid sites (coordinatively unsaturated Zr, Zr_{cus}) and Brønsted acid sites (bridging hydroxyls between three Zr atoms, or functionalized linkers) that have been cited as critical in catalytic processes and enhanced proton mobility.[6-10]

MOFs contain intrinsic acid sites useful for adsorption, separation and catalysis. Improvements to materials for gas storage and separation have been previously identified through tuning reactive metal centers or functionalized ligands that bind to gas molecules.[11-14] For instance, a recent study by Andonova et al. found that the incorporation of excess hydroxyl groups onto MIL-53-Al improved CO_2 adsorption capacity relative to the non-functionalized material.[15] Recent research has focused on the importance of hydrogen bonding for gas adsorption and separation between the native hydroxyl groups in many of these porous materials and small molecules such as CO, CO_2, SO_2, NO_2, and organic compounds.[15-20] However, a molecular-level understanding of the energetics of small molecule adsorption, like CO, is still lacking.

One of the most widely studied Zr-MOFs, UiO-66, contains a $Zr_6(OH)_4O_4$ core that is coordinated to 12 benzene-1,4 dicarboxylate (BDC) linkers (See Fig. 1). The ideal structure of UiO-66 contains four Brønsted acid sites per Zr node in the form of μ_3-OH groups on alternating faces of the Zr_6 octahedron. These bridging hydroxyls reside at the corners of the MOF's tetrahedral cavity.[21] Klet et al. calculated the pKa of the μ_3-OH proton to be 3.52.[22] FTIR measurements of adsorbed CO have been utilized to suggest that the μ_3-OH of UiO-66 is considered a weak Brønsted acid.[23] These studies have led many in the field to speculate that the bridging hydroxyls between two identical metal atoms have limited acidity and thus limited adsorption capability.[24] In fact, the functionalization of MOFs to generate stronger Brønsted acid

sites has garnered significant attention.[24-27] Yet, the addition of functionality through the incorporation of sulfates onto the MOF greatly enhances the Brønsted acidity of the bridging and terminal hydroxyls.[28] While the community is making progress in answering fundamental questions about acidic sites in MOFs, a more complete understanding of the interactions between small molecules, like CO and these type of sites in the well-studied UiO-66 is needed.

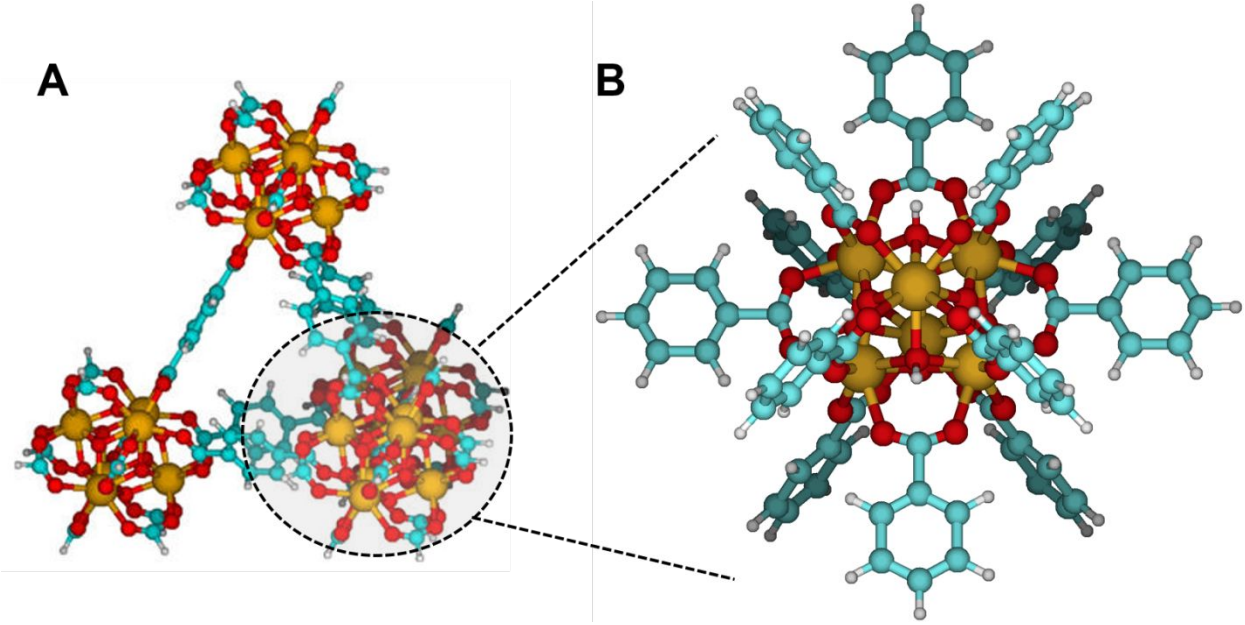

Figure 1. Illustration of the tetrahedral pore environment (A) and the Zr_6 node + 12 linkers (B) with the μ_3-OH facing upwards of UiO-66. The zirconium, oxygen, carbon, and hydrogen atoms are shown in yellow, red, blue, and white respectively.

The energetics of CO adsorption onto surface hydroxyl groups has been previously studied through the utilization of *in situ* vibrational spectroscopy.[29-31] When gas molecules of CO bind to hydroxyl sites, the shift in vibrational frequency of both the Zr-MOF hydroxyl, $\Delta\nu$(OH), and the adsorbate, $\Delta\nu$(CO), give insight into the geometry and strength of the CO-hydroxyl interaction.[23,32-35] Using shifts in the infrared vibration of adsorbed CO, Storozhev et al. found amphipathic behavior when CO interacted with silanol groups in amorphous silica through either the carbon or oxygen ends.[31] In addition to the binding geometries, the adsorption energetics of CO-hydroxyl interactions have been experimentally attained on a variety of porous materials via *in situ* spectroscopic measurements at variable temperatures.[29-31,36,37] While

the scientific community has spent the past thirty years studying CO adsorption onto hydroxyl groups, there has yet to be a systematic evaluation of geometries and energetics associated with CO adsorption onto the hydroxyl groups of the most ubiquitous MOF studied–UiO-66. Measurements of CO adsorption on to specific surface sites provide clear chemical and electronic structural characterization of the surface species, which is important for continued progress in the field of MOF-enabled small molecule adsorption and separation.

We have applied *in situ* infrared spectroscopy in combination with electronic structure calculations to investigate CO adsorption sites and geometries on the surface of UiO-66. Previously, our research has focused on CO interactions with the coordinatively unsaturated Zr sites that arise from missing linker defects in UiO-66.[38] In this manuscript, we applied a similar experimental approach to characterize CO-hydroxyl intermolecular interactions. The studies presented herein describe the arrangement and energetics between CO and the μ_3-OH groups of UiO-66, while also laying the groundwork for future studies to probe Brønsted acidity in Zr-based MOFs.

II. Methods

UiO-66 Synthesis. The synthesis of low defect density UiO-66 was based on an established literature procedure.[39] $ZrCl_4$ (378 mg, 1.62 mmol) and terephthalic acid (539 mg, 3.24 mmol) were suspended in dimethylformamide (DMF) (10 mL) inside a 6 dram vial. 37 % HCl (0.286 mL, 3.24 mmol) was added to the reaction mixture and stirred at 343 K for 30 min to ensure complete dissolution of the starting materials. The resultant solution was transferred into a Teflon-lined Parr reactor, which was heated at 493 K for 24 hours. After cooling to room temperature, a white powder was isolated by centrifugation, washed with fresh DMF (4 × 10 mL), and then soaked in DMF (10 mL) for 4 days. The solvent was replaced every 24 hours. The resultant framework was dried in air at 333 K for 24 hours, followed by 473 K for 1 hour. The MOF powder was further washed with acetone using a Soxhlet extractor for 24 hours followed by drying in air at 473 K for 1 hour.

Infrared Studies of Adsorption. Infrared spectroscopic experiments were performed in a stainless-steel high vacuum cell with a base pressure of 1×10^{-8} Torr. The UiO-66 sample was pressed as a 7 mm disk into a tungsten mesh, which was then clamped onto a precision manipulator. Previous characterization suggests no structural change to the underlying UiO-66 framework as a result of a pelletization pressure up to 10,000 psi.[40] The resistively heated tungsten mesh attached to an external power supply and cooled using a liquid-nitrogen reservoir provided the necessary heating and cooling measures for experimentation. A K-type thermocouple, spot welded directly to the mesh, monitored the sample temperature. Details on this high vacuum experimental cell can be found in a previous study.[41] For infrared analysis, we employed an FTIR spectrometer (Thermo, Nicolet Nexus 470 FTIR) mounted on the side of the vacuum chamber with an external MCT-A detector and spectral resolution of 2 cm^{-1}.

Vacuum annealing of samples at 473 K effectively removed weakly bound adsorbates for each experiment. The dehydroxylation of UiO-66 required a pretreatment temperature of 573 K, which easily removed the μ_3-hydroxyls located in the tetrahedral cavities of the MOF without the formation of defects.[38] A filter (NANOCHEM Purifilter, Matheson Tri Gas) was attached to the manifold to remove any metal carbonyls from the gas stream. CO (Airgas, 99.3%) was systematically introduced at 183 K and equilibrated within the vacuum chamber at pressures ranging from 50 mTorr to 4 Torr.

Variable-Temperature Infrared Spectroscopy. Variable-temperature infrared spectroscopic (VTIR) measurements characterized the energetics of CO-surface interations.[36] VTIR requires a fixed partial pressure of CO interacting with the UiO-66 sample within a closed system. The equilibrium constant for CO adsorption depends on temperature according to the van't Hoff equation:

$$\ln K(T) = \left(-\frac{\Delta H^{\circ}_{ads}}{RT}\right) + \left(\frac{\Delta S^{\circ}_{ads}}{R}\right) \qquad (1)$$

where K is the equilibrium constant of the adsorption process while both ΔH°_{ads} and ΔS°_{ads} are temperature independent values of the standard enthalpy and entropy of adsorption, respectively.

The VTIR method utilizes the assumption of Langmuirian adsorption for CO gas phase molecules. The fractional coverage of CO on the surface, θ, defined by the Langmuir adsorption model is related to the intensity of the characteristic CO-surface IR absorption band, A. Within this construct, one can express surface coverage as:

$$\theta = \frac{A}{A_M} = \frac{\exp\left[\frac{\Delta S^{\circ}_{ads}}{\mathrm{R}}\right]\exp\left[-\frac{\Delta H^{\circ}_{ads}}{RT}\right]p}{(1 + \exp\left[\frac{\Delta S^{\circ}_{ads}}{\mathrm{R}}\right]\exp\left[-\frac{\Delta H^{\circ}_{ads}}{RT}\right]p)} \qquad (2)$$

where A_M is the intensity under full coverage of CO on the surface site and p is the pressure of the closed system.

Experimentally, the energetics of CO-surface interactions were attained by introducing 4 Torr of CO into the vacuum chamber at 183 K. Following CO introduction, the sealed chamber equilibrated at a given temperature for a ten-minute period prior to data collection. The acquisition of infrared spectra ranged from 183 K – 233 K and composed of an average of 250 scans.

Computational Details. Determination of the binding geometry and energy of CO on the μ_3-OH groups of UiO-66 used a fully relaxed cluster model of UiO-66 consisting of a $Zr_6(OH)_4O_4$ capped by 12 benzoate ligands with heavy atoms frozen at the experimental crystallographic coordinates. Geometry optimizations and harmonic vibrational frequency calculations were carried out with the M06-L functional[42] using a 6-31G* basis set for C, O, and H atoms of the cluster and ligands other than the μ_3-OH and CO adsorbate, an aug-cc-pVTZ basis set for the μ_3-OH and CO atoms, and the Lanl2dz basis set and pseudopotentials for Zr atoms. Using these geometries, single point calculations with the M06-2X functional[43] and the same basis set were conducted to further refine the electronic energies, which were corrected by the basis set superposition error using the counterpoise scheme. All calculation incorporated a superfine integration grid. The reported energetic data correspond to adsorption enthalpies at 200 K.

III. Results and Discussion

CO adsorption on UiO-66 has been characterized via infrared spectroscopy of adsorbed CO. The unique vibrational character of adsorbed CO not only probes the molecular nature of acidic sites,[23,38,44-46] but also provides the thermodynamics of CO uptake and transport within materials.[29,36,47,48] Rational development of next-generation materials for the sorption and separation of small gas molecules, such as CO, requires a fundamental understanding of the interactions between the abundant hydroxyl groups of materials and the gas molecules of interest.[16,18,23,24] Hydroxyl–CO interactions result from electrostatic forces that cause significant perturbation to the vibrational stretching frequency of the C-O bond. In addition, the vibrational frequency of CO provides insight into the binding geometry and specifically the orientation of CO adsorption (through the C- end or the O- end of the adsorbate).[32] The binding complexity of CO adsorption and the applications in small molecule adsorption stimulate the detailed studies we present below.

Characterization of UiO-66. Infrared spectroscopic characterization of the synthesized UiO-66 material, shown in Figure 2, revealed that the MOF retained sharp, narrow spectroscopic features associated with the linker vibrational motions in vacuum and following a thermal treatment at 473 K. The full width at half max (FWHM) of the linker vibrational band assigned to the aromatic breathing motion (1020 cm^{-1} vibration with a FWHM ~10 cm^{-1}) indicated that UiO-66 retained a framework structure under the high vacuum experimental conditions.[17,49] In addition to the carbon-containing linker vibrations, the sharp vibrational feature at 3674 cm^{-1} has been identified as the μ_3-hydroxyl groups of the zirconium nodes located in the tetrahedral cavity (Figure 2, black trace).[17,49] Some organics remained bound to the framework, as evidenced by the broad feature associated with hydroxyl groups at 3400 cm^{-1} and three infrared absorbance bands at 2921 cm^{-1}, 2852 cm^{-1} and 1732 cm^{-1}. We speculate that residual formate and acetone from sample preparation remained adsorbed to the μ_3-OH groups of UiO-66. These contaminates act as spectator species for the CO adsorption studies presented herein and are removed upon an increase in the sample pretreatment temperature to 573 K (Figure 2, red trace). The increase in the vacuum pretreatment temperature to 573 K resulted in the rapid desorption of water from the material and produced

the dehydroxylated form of UiO-66. The infrared spectrum of the dehydroxylated UiO-66 material showed a significant depletion of the 3674 cm^{-1} feature while retaining the sharp vibrational features of the organic linkers. These results are consistent with previously acquired TGA and PXRD patterns that suggest the underlying framework remains intact at temperatures up to 573 K in vacuum.[38,40]

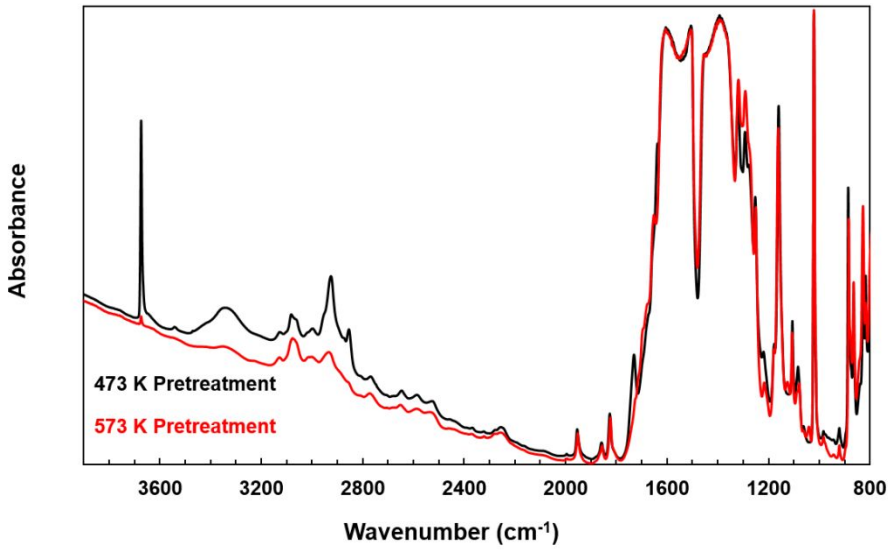

Figure 2. Infrared spectra of the MOF, UiO-66, acquired after pretreatment temperatures of 473 K (black) and 573 K (red).

CO Adsorption on UiO-66. Adsorbed CO is an excellent probe molecule due to the sensitivity of $\nu(C\text{-}O)_{ads}$ when the adsorbate interacts with acidic binding sites on MOFs.[15,23,38,50] Carbon monoxide adsorption was performed under varying CO pressures at 183 K, a temperature low enough to achieve extended surface residence time. Infrared spectra of CO adsorption, shown in Figure 3, were recorded *in situ* and referenced to the clean UiO-66. Upon CO exposure at 50 mTorr (Figure 3B), two prominent features appeared at 2152 cm^{-1} and 2124 cm^{-1}. As the pressure of CO increased inside the chamber, the integrated area under both the 2152 cm^{-1} and 2124 cm^{-1} features increased. The large positive absorbance feature at 2152 cm^{-1} has been previously proposed to be CO interacting with μ_3-hydroxyl groups through the carbon end of the adsorbate (ZrOH···CO).[23] The interaction between CO and the μ_3-OH is electrostatic

and the magnitude of the change in vibrational frequency compared to the gas phase fundamental vibration at 2143 cm^{-1} [$\Delta\nu$(CO)] depends on the strength of the electrostatic field according to the Stark effect.[46] The observed CO stretching frequency on UiO-66 agrees with previous reported studies of CO binding to hydroxylated surfaces such as silicates and zirconia.[29,31,32,51]

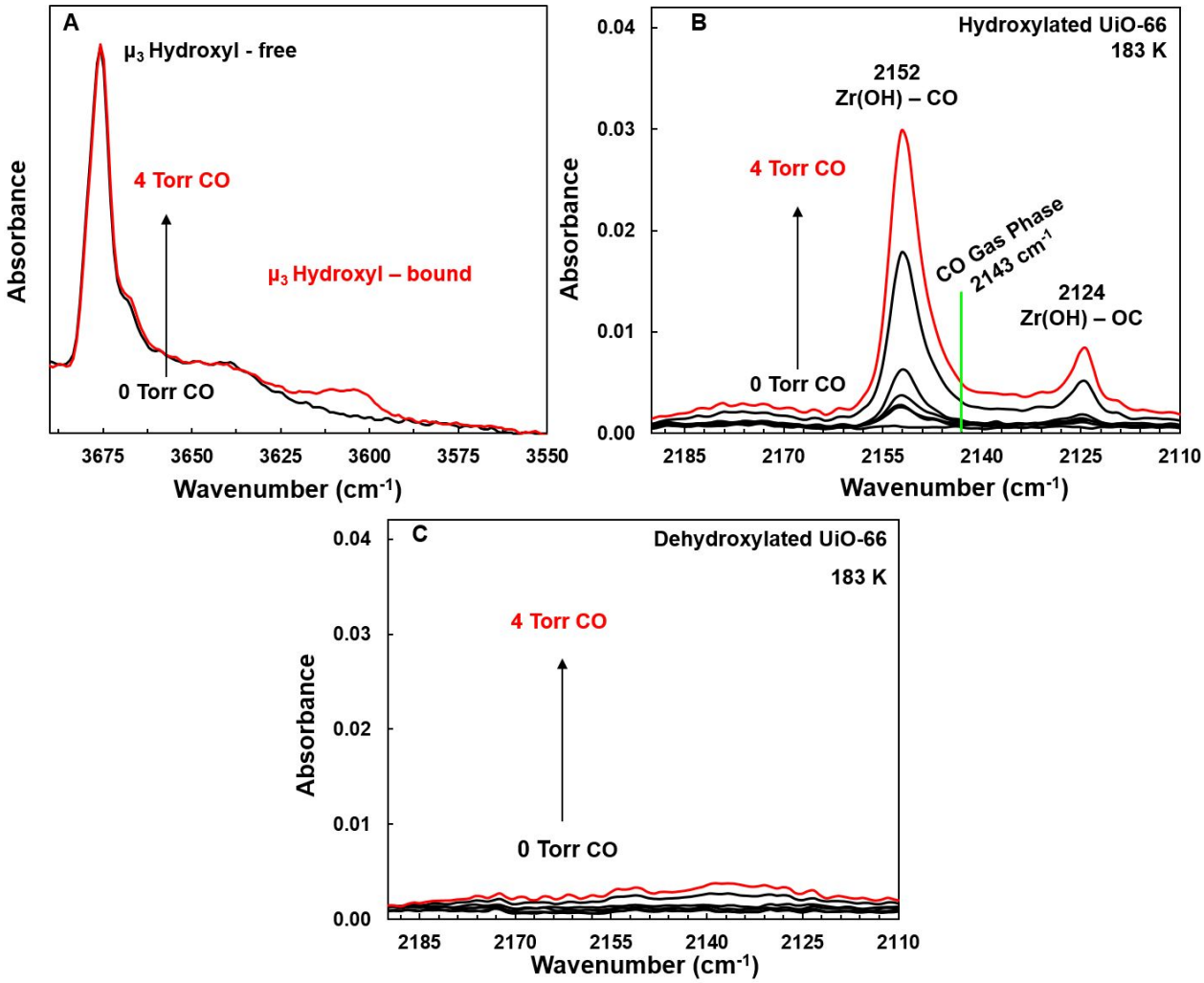

Figure 3. Infrared spectra of CO adsorption at increasing pressures ranging from 0 Torr up to 4 Torr on hydroxylated UiO-66 in the hydroxyl stretching region (A) and C-O stretching region (B). (C) Infrared spectra of CO adsorption under the same experimental conditions on dehydroxylated UiO-66.

Unlike the 2152 cm^{-1} CO-hydroxyl feature, the CO-MOF vibrational feature at 2124 cm^{-1} (shown in Figure 3B) has not been previously reported for CO uptake within UiO-66. The observed infrared feature redshifted 19 cm^{-1} from the gas phase fundamental frequency of CO. We hypothesize that this redshift is

due to a μ_3-OH···OC binding geometry. This isocarbonyl binding configuration is most commonly observed spectroscopically when CO interacts with alkali-metal cations in zeolites,[46,52] and has also been identified in CO adsorption onto hydroxyl groups of silica[31] and the MOF, MIL-53.[33]

Analogous experiments with the dehydroxylated UiO-66 framework verified the assignment of the 2124 cm^{-1} feature in the infrared absorption spectrum to the μ_3-OH···OC binding geometry. Upon CO exposure to the dehydroxylated UiO-66 sample at identical concentrations of CO within the chamber, both vibrational features at 2152 cm^{-1} and 2124 cm^{-1} remained absent in the infrared difference spectra (Figure 3C). The absence of CO vibrational features upon dehydroxylation of UiO-66 suggests the μ_3-hydroxyl is required for the small molecule to bind within tetrahedral cavities (the location of the μ_3-OH groups) of the porous structure. In addition, these studies provide evidence that weakly-bound physisorbed CO molecules are not present, in measureable quantities, under our experimental conditions. The dehydroxylated UiO-66 studies also lend support to the attribution of the 2124 cm^{-1} vibration to CO interacting with the μ_3-OH groups through the oxygen atom.

Infrared spectroscopy of the high wavenumber region (> 3000 cm^{-1}) confirms the presence of the CO–hydroxyl interaction and also provides insight into the acidity of the MOF hydroxyl. Perturbation of the free μ_3-hydroxyl groups identified the presence of CO on UiO-66 as a small, broad feature at 3605 cm^{-1} (Figure 3A). The feature at 3605 cm^{-1} is attributed to a hydrogen bonded μ_3-hydroxyl vibration redshifted relative to the free OH band at 3674 cm^{-1}. The asymmetric nature of the bound-hydroxyl feature could be credited to both the OH···CO, centered at 3605 cm^{-1}, and a second feature centered at 3620 cm^{-1} associated with the OH···OC binding configuration. Recent studies illustrate the proton affinity of the hydroxyl groups can be directly related to the redshift in the ν(OH) upon exposure to CO.[32,35] Our data indicate that the bridging hydroxyls of UiO-66 are only weakly acidic, consistent with previous investigations of UiO-66 acidity[23] as well as type I zirconium hydroxides.[51]

Energetics of CO – Hydroxyl Interactions. The binding energetics of CO on the μ_3-hydroxyl groups of UiO-66 were measured utilizing variable temperature infrared spectroscopy (VTIR). The

introduction of 4 Torr of CO adsorbed onto UiO-66 over a wide range of temperatures provided a closed gas-surface system to initiate the van't Hoff analysis. The infrared spectra acquired at each temperature are shown in Figure 4A. As the temperature of the sample increased, the equilibrium between $CO_{(ads)}$ and $CO_{(g)}$ shifted to the gas phase and the CO-μ_3 hydroxyl concentration diminished.

The energetics of the CO-hydroxyl interaction were quantified through a van't Hoff analysis of the VTIR experimental data. This analysis has been shown to be highly successful in characterizing gas-surface binding energetics in a number of studies, and reviewed here.[36] In this study, we increased the temperature of the sample while acquiring infrared spectra at each temperature and subsequently observed a decrease in the concentration of CO$\cdots\mu_3$-OH interactions, shown in Figure 4. No measurable pressure increases within the chamber accompanied the decrease in concentration of the CO$\cdots\mu_3$-OH configuration. As a result, the relationship between integrated absorbance and the standard enthalpy of adsorption ($\Delta H°_{ads}$) eqn. 2 can be written as:

$$A \approx A_M \exp\left[-\frac{\Delta S°_{ads}}{R}\right] N_{tot}\left(\frac{RT}{V_g}\right) e\exp\left[-\frac{\Delta H°_{ads}}{RT}\right] \propto T \exp\left[-\frac{\Delta H°_{ads}}{RT}\right] \quad (3)$$

where N_{tot} is the total number of adsorbate moles in the system (both in the gas phase and adsorbed) within a fixed volume, V_g. From this point, we assume the surface coverage is negligible ($\theta \ll 1$) and only $\Delta H°_{ads}$ can be evaluated.

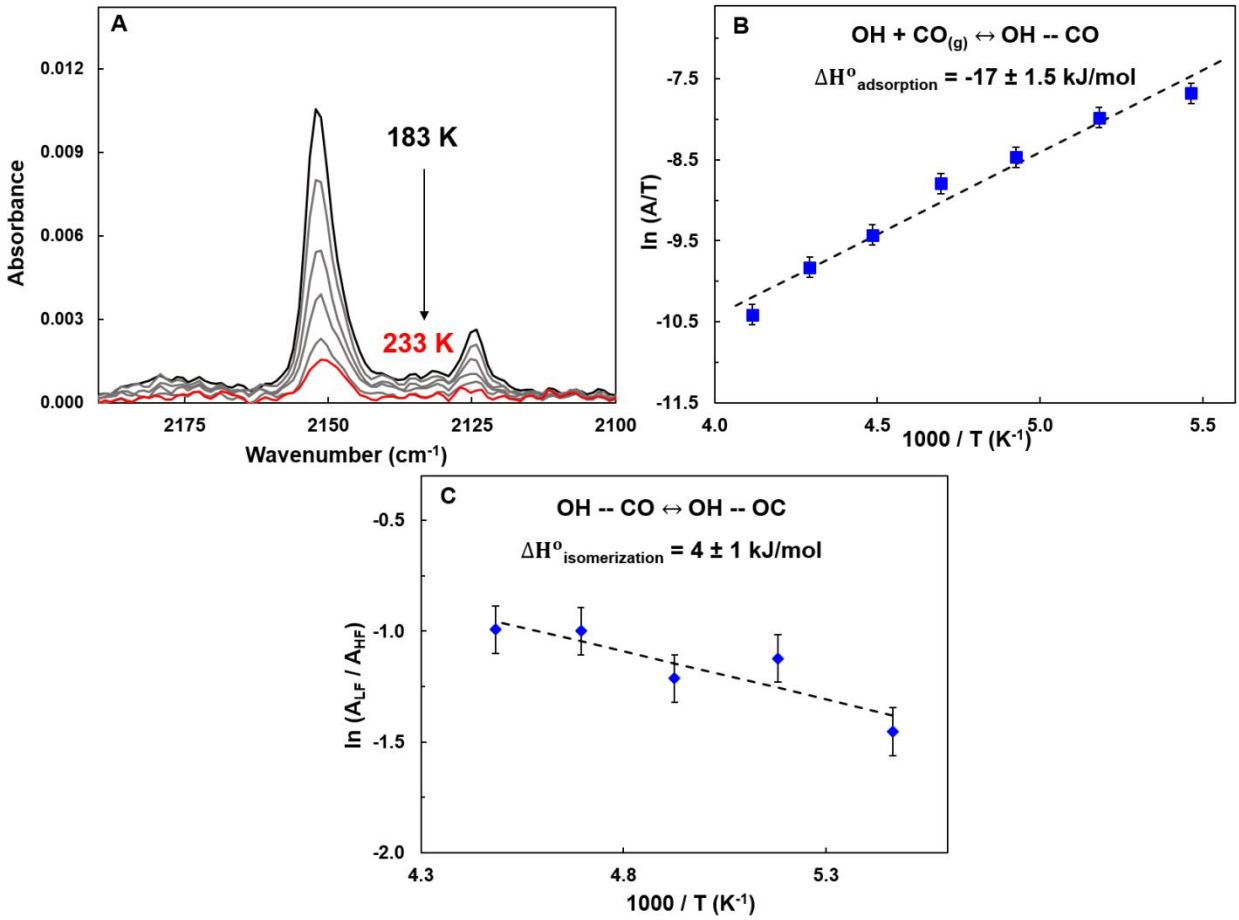

Figure 4. CO adsorption on UiO-66 under varying temperatures in a closed equilibrium environment. Panel A provides the infrared spectra acquired at each temperature (183 K, 193 K, 203 K, 213 K, 223 K and 233 K). Panel B provides a van't Hoff plot of the integrated absorbance of the 2152 cm^{-1} ZrOH ··· CO feature with the linear slope to provide $\Delta H°_{adsorption}$. Panel C is the ratio of the natural log of the integrated absorbance of the 2124 cm^{-1} and 2152 cm^{-1} CO features. A linear slope is provided to calculate the $\Delta H°_{isomerization}$. Error bars represent the standard deviation of triplicate data points.

Figure 4B provides a van't Hoff plot and, under the assumption of low surface coverage, the standard enthalpy of adsorption for the ZrOH···CO interaction was found to be -17 ± 1.5 kJ/mol. The experimentally attained $\Delta H°_{ads}$ for the ZrOH···CO agrees with the energetics of other weak Brønsted acid–CO interactions including silica (-11 kJ/mol $\Delta H°_{ads}$)[29] and H-ZSM-5 (-25.5 kJ/mol $\Delta H°_{ads}$).[37] The relatively weak standard enthalpy of adsorption, as determined by VTIR, for the ZrOH···CO interaction is consistent with previous adsorption calorimetry experiments for CO on UiO-66 that were observed to be between 16.0

and 16.6 kJ/mol.[23] The main adsorption pathway for CO on a non-defective UiO-66 framework occurs through the μ_3-OH group. However, CO interacts weakly compared to the CO interactions with coordinatively unsaturated metal sites (calculated binding energy of 81 kJ/mol on Zr_{cus}).[38]

In addition to the energetics of CO adsorption, VTIR can be employed to investigate the enthalpic difference between CO bound through the carbon and oxygen atoms.[36] In the closed chamber environment, an increase in temperature of the material resulted in the concentrations of both the μ_3OH···CO geometry (referred to as high frequency: HF) and the low frequency (LF) μ_3OH···OC geometry to decrease. However, the ratio of A_{LF}/A_{HF} increased over that same range and therefore provided the enthalpic energy difference ($\Delta H°_{iso}$) from the more energetically stable carbonyl configuration to isocarbonyl configuration (μ_3OH···CO ↔ μ_3OH···OC). Integration of both the HF and the LF CO features is used to determine the standard enthalpy of isomerization, $\Delta H°_{iso}$, as shown below[36]:

$$\ln\left(\frac{A_{LF}}{A_{HF}}\right) = \left(-\frac{\Delta H^{\circ}_{iso}}{RT}\right) + \left(\frac{\Delta S^{\circ}_{iso}}{R}\right) + \ln\left(\frac{\varepsilon_{LF}}{\varepsilon_{HF}}\right) \qquad (4)$$

where ε represents the molar extinction coefficient for each CO vibration. The relationship between $1/T$ and $\ln(A_{LF}/A_{HF})$ (shown in Fig. 4C) identifies the isomerization enthalpy as 4 ± 1 kJ/mol while the ΔS°_{iso} cannot be attained without molar extinction coefficients for each unique CO–surface vibration.

The strength and binding geometries of the CO···μ_3-hydroxyl interaction were further explored computationally. Figure 5 shows calculated structures of CO hydrogen bonding to the μ_3-OH group of UiO-66 through its carbon and oxygen ends. The calculations also predicted the experimentally confirmed blueshift in vibrational frequency for the ν(CO) vibration when bound through the carbon atom (2179 cm^{-1}) and redshift when bound through the oxygen atom (2121 cm^{-1}, both consider a 0.9744 scaling factor obtained from the ratio of the experimental to calculated gas-phase CO stretch at the same level of theory). We have performed DFT calculations of the bridging-OH---CO hydrogen bond in a side-on configuration. However, a stable minimum could not be identified in that orientation. The enthalpies of adsorption computed at 200 K for each calculated geometry, corrected by the basis set superposition error, were also

calculated to be -31.8 kJ/mol and -21.8 kJ/mol for the μ_3-OH···OC and μ_3-OH···CO configurations, respectively. While the relative strength of the two binding geometries measured by the experiment is nicely captured by the calculations, the calculated enthalpies overestimate the measured values by 8-15 kJ/mol, indicating incompleteness of the basis set, inadequacy of the DFT functional chosen to recover all electron correlation, or a combination of both.

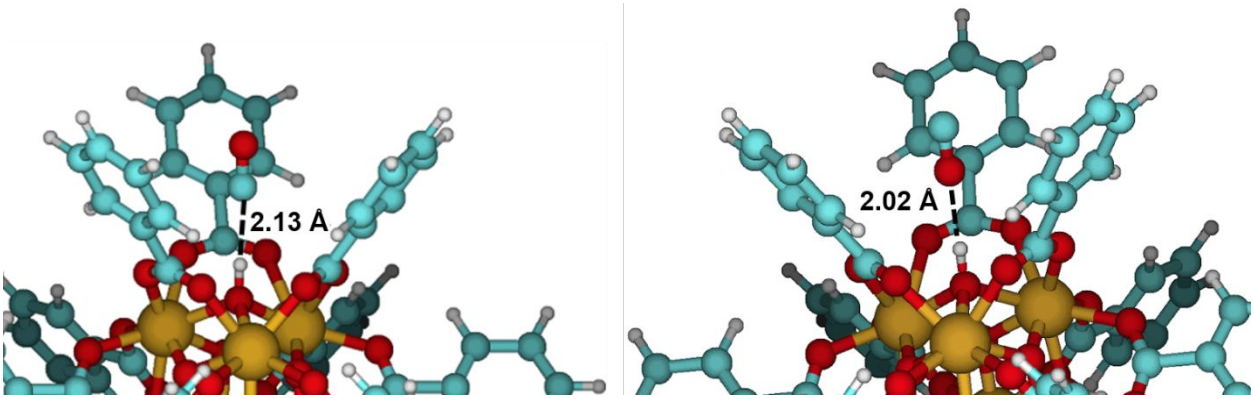

Figure 5. Calculated geometries of CO hydrogen bonding to a μ_3-OH site through its carbon end (a) and through its oxygen end (b). The Zr, O, H, and C atoms are shown in gold, red, white, and teal respectively.

The spectroscopic analysis of CO interacting with UiO-66, in conjunction with DFT calculations, provides clear evidence of unique geometries and energetics of two well-resolved adsorption events that are mediated by selective binding to the weakly acidic μ_3-OH groups located within tetrahedral cavities of the MOF UiO-66. As new materials are produced for gas storage and transport applications, variable-temperature spectroscopic methods can help identify binding configurations and provide energetic information for each specific site. These studies will help identify and optimize materials capable of increased sorption capacity for a specific small molecule.

IV. Summary

In situ infrared spectroscopy and computational measurements provided evidence of CO hydrogen bonding to the μ_3-hydroxyl of UiO-66. CO hydrogen bonds to the μ_3-hydroxyl through electrostatic interactions in which the CO stretching frequency is perturbed due to the Stark effect, induced primarily by

the MOF's μ_3-OH group. CO interacts with the μ_3-hydroxyl through both the carbon atom and oxygen atom as evidenced by two unique stretching frequencies for ZrOH···CO and ZrOH···OC. Upon dehydroxylation of UiO-66, both CO binding geometries are absent—confirming the significance of hydroxyl-CO interactions to the sorption of CO within UiO-66. A van't Hoff analysis of the CO-hydrogen bond suggests a $\Delta H°_{adsorption}$ of -17 kJ/mol and an isomerization pathway (from carbonyl to isocarbonyl) with a $\Delta H°_{isomerization}$ of 4 kJ/mol. We show that the VTIR methodology is an exceptional experimental benchmark for computational-based studies on small molecule–hydroxyl interactions within MOFs. Finally, the vibrational shifts of the CO–μ_3-OH interaction suggest that small molecules can characterize acidity of hydroxyls and provide fundamental insight into binding energetics—critical in initial development of new materials for small molecule sorption and separation.

Conflicts of Interest

There are no conflicts of interest to declare.

Acknowledgements

This material is based upon work supported by the U.S. Army Research Laboratory and the U.S. Army Research Office under Grant No. W911NF-15-2-0107. We are grateful for support of the Defense Threat Reduction Agency under Program No. BB11PHM156. The work of A. J. Morris and P. M. Usov was supported by the U.S. Department of Energy (DOE), Office of Basic Energy Sciences, under Award Number DE-SC0012445. The authors acknowledge Advanced Research Computing at Virginia Tech for providing computational resources and technical support that have contributed to the results reported within this paper.

TOC

Fundamental studies of CO adsorption on UiO-66 reveal adsorption occurs through interactions with the μ_3-OH groups and once bound, CO binds through both the C- and O- end of the molecule.

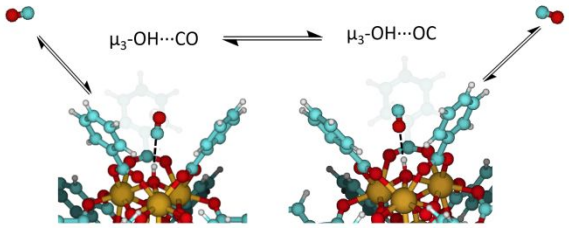

References

1. N. S. Bobbitt, M. L. Mendonca, A. J. Howarth, T. Islamoglu, J. T. Hupp, O. K. Farha and R. Q. Snurr, Chem. Soc. Rev., 2017, 46, 3357-3385.
2. M. Taddei, Coord. Chem. Rev., 2017, 343, 1-24.
3. Z. Fang, B. Bueken, D. E. De Vos and R. A. Fischer, Angew. Chem. Int. Ed., 2015, 54, 7234-7254.
4. J. Canivet, M. Vandichel and D. Farrusseng, Dalton Transactions, 2016, 45, 4090-4099.
5. J. Ren, M. Ledwaba, N. M. Musyoka, H. W. Langmi, M. Mathe, S. Liao and W. Pang, Coord. Chem. Rev., 2017, 349, 169-197.
6. M. Rimoldi, A. J. Howarth, M. R. DeStefano, L. Lin, S. Goswami, P. Li, J. T. Hupp and O. K. Farha, ACS Catal., 2017, 7, 997-1014.
7. F. Vermoortele, R. Ameloot, A. Vimont, C. Serre and D. De Vos, Chem. Commun., 2011, 47, 1521-1523.
8. Y. Liu, R. C. Klet, J. T. Hupp and O. Farha, Chem. Commun., 2016, 52, 7806-7809.
9. J. M. Taylor, S. Dekura, R. Ikeda and H. Kitagawa, Chem. Mater., 2015, 27, 2286-2289.
10. C. Ardila-Suarez, S. Perez-Beltran, G. E. Ramirez-Caballero and P. B. Balbuena, Catal. Sci. Technol., 2018, 8, 847-857.
11. K. Sumida, D. L. Rogow, J. A. Mason, T. M. McDonald, E. D. Bloch, Z. R. Herm, T.-H. Bae and J. R. Long, Chem. Rev., 2012, 112, 724-781.
12. S. M. Cohen, Chem. Rev., 2012, 112, 970-1000.
13. A. Evans, R. Luebke and C. Petit, J. Mater. Chem. A, 2018, 6, 10570-10594.
14. C. Campbell, J. R. B. Gomes, M. Fischer and M. Jorge, J. Phys. Chem. Lett., 2018, 9, 3544-3553.
15. S. Andonova, E. Ivanova, J. Yang and K. Hadjiivanov, J. Phys. Chem. C, 2017, 121, 18665-18673.
16. K. Tan, S. Zuluaga, E. Fuentes, E. C. Mattson, J.-F. Veyan, H. Wang, J. Li, T. Thonhauser and Y. J. Chabal, Nature Communication, 2016, 7, 13871.
17. C. H. Sharp, J. Abelard, A. M. Plonka, W. Guo, C. L. Hill and J. R. Morris, J. Phys. Chem. C, 2017, 121, 8902-8906.
18. K. Tan, S. Jensen, S. Zuluaga, E. K. Chapman, H. Wang, R. Rahman, J. Cure, T.-H. Kim, J. Li, T. Thonhauser and Y. J. Chabal, J. Am. Chem. Soc., 2018, 140, 856-859.
19. T. G. Grissom, C. H. Sharp, P. M. Usov, D. Troya, A. J. Morris and J. R. Morris, J. Phys. Chem. C, 2018, 122, 16060-16069.

20. W. Zhang, Y. Ma, I. A. Santos-López, J. M. Lownsbury, H. Yu, W.-G. Liu, D. G. Truhlar, C. T. Campbell and O. E. Vilches, J. Am. Chem. Soc., 2018, 140, 328-338.
21. J. H. Cavka, S. Jakobsen, U. Olsbye, N. Guillou, C. Lamberti, S. Bordiga and K. P. Lillerud, J. Am. Chem. Soc., 2008, 130, 13850-13851.
22. R. C. Klet, Y. Liu, T. C. Wang, J. T. Hupp and O. K. Farha, J. Mater. Chem. A, 2016, 4, 1479-1485.
23. A. D. Wiersum, E. Soubeyrand-Lenoir, Q. Yang, B. Moulin, V. Guillerm, M. B. Yahia, S. Bourrelly, A. Vimont, S. Miller, C. Vagner, M. Daturi, G. Clet, C. Serre, G. Maurin and P. L. Llewellyn, Chemistry – An Asian Journal, 2011, 6, 3270-3280.
24. J. Jiang and O. M. Yaghi, Chem. Rev., 2015, 115, 6966-6997.
25. J. B. DeCoste, T. J. Demasky, M. J. Katz, O. K. Farha and J. T. Hupp, New J. Chem., 2015, 39, 2396-2399.
26. M. J. Katz, Z. J. Brown, Y. J. Colon, P. W. Siu, K. A. Scheidt, R. Q. Snurr, J. T. Hupp and O. K. Farha, Chem. Commun., 2013, 49, 9449-9451.
27. H. Furukawa, F. Gándara, Y.-B. Zhang, J. Jiang, W. L. Queen, M. R. Hudson and O. M. Yaghi, J. Am. Chem. Soc., 2014, 136, 4369-4381.
28. J. Jiang, F. Gándara, Y.-B. Zhang, K. Na, O. M. Yaghi and W. G. Klemperer, J. Am. Chem. Soc., 2014, 136, 12844-12847.
29. T. P. Beebe and J. T. Yates, Surf. Sci., 1985, 159, 369-380.
30. M. R. Delgado, R. Bulánek, P. Chlubná and C. O. Arean, Catal. Today, 2014, 227, 45-49.
31. P. Y. Storozhev, C. Otero Areán, E. Garrone, P. Ugliengo, V. A. Ermoshin and A. A. Tsyganenko, Chem. Phys. Lett., 2003, 374, 439-445.
32. K. Hadjiivanov, in Advances in Catalysis, ed. F. C. Jentoft, Academic Press, 2014, vol. 57, pp. 99-318.
33. U. Ravon, G. Chaplais, C. Chizallet, B. Seyyedi , F. Bonino , S. Bordiga , N. Bats and D. Farrusseng, ChemCatChem, 2010, 2, 1235-1238.
34. M. L. Hair and W. Hertl, J. Phys. Chem., 1970, 74, 91-94.
35. A. P. Evgenii and E. N. Yurchenko, Russian Chemical Reviews, 1983, 52, 242.
36. E. Garrone and C. Otero Arean, Chem. Soc. Rev., 2005, 34, 846-857.
37. C. Otero Areán, Olga V. Manoilova, Alexey A. Tsyganenko, G. Turnes Palomino, M. Peñarroya Mentruit, F. Geobaldo and E. Garrone, Eur. J. Inorg. Chem., 2001, 2001, 1739-1743.
38. D. M. Driscoll, D. Troya, P. M. Usov, A. J. Maynes, A. J. Morris and J. R. Morris, J. Phys. Chem. C, 2018, 122, 14582-14589.
39. G. C. Shearer, S. Chavan, S. Bordiga, S. Svelle, U. Olsbye and K. P. Lillerud, Chem. Mater., 2016, 28, 3749-3761.
40. G. W. Peterson, J. B. DeCoste, T. G. Glover, Y. Huang, H. Jasuja and K. S. Walton, Microporous Mesoporous Mater., 2013, 179, 48-53.
41. P. Basu, T. H. Ballinger and J. T. Yates, Rev. Sci. Instrum., 1988, 59, 1321-1327.
42. Y. Zhao and D. G. Truhlar, J. Chem. Phys., 2006, 125, 194101.
43. Y. Zhao and D. G. Truhlar, Theor. Chem. Acc., 2008, 120, 215-241.
44. I. X. Green, W. J. Tang, M. Neurock and J. T. Yates, Science, 2011, 333, 736-739.
45. R. Eischens, W. Pliskin and S. Francis, J. Chem. Phys., 1954, 22, 1786-1787.
46. K. I. Hadjiivanov and G. N. Vayssilov, in Advances in Catalysis, Vol 47, eds. B. C. Gates and H. Knozinger, Elsevier Academic Press Inc, San Diego, 2002, vol. 47, pp. 307-511.
47. M. R. Delgado, A. M. de Yuso, R. Bulánek and C. O. Arean, Chem. Phys. Lett., 2015, 639, 195-198.
48. C. Otero Areán, A. A. Tsyganenko, E. Escalona Platero, E. Garrone and A. Zecchina, Angew. Chem. Int. Ed., 1998, 37, 3161-3163.
49. G. Wang, C. Sharp, A. M. Plonka, Q. Wang, A. I. Frenkel, W. Guo, C. Hill, C. Smith, J. Kollar, D. Troya and J. R. Morris, J. Phys. Chem. C, 2017, 121, 11261-11272.

50. N. Drenchev, M. Mihaylov, P. D. C. Dietzel, A. Albinati, P. A. Georgiev and K. Hadjiivanov, J. Phys. Chem. C, 2016, 120, 23083-23092.
51. K. Hadjiivanov and J.-C. Lavalley, Catal. Commun., 2001, 2, 129-133.
52. O. V. Manoilova, M. Peñarroya Mentruit, G. Turnes Palomino, A. A. Tsyganenko and C. Otero Areán, Vib. Spectrosc, 2001, 26, 107-111.